SH 2.1-13

ABUNDANCES FROM SOLAR-FLARE GAMMA-RAY LINE SPECTROSCOPY

R. J. Murphy
University of Maryland
College Park, MD 20742

R. Ramaty
NASA/GSFC
Greenbelt, MD 20771

D. J. Forrest
University of New Hampshire
Durham, NH 03824

B. Kozlovsky
Tel Aviv University
Tel Aviv, ISRAEL

ABSTRACT

Elemental abundances of the ambient gas at the site of gamma-ray line production in the solar atmosphere are deduced using gamma-ray line observations from a solar flare. The resultant abundances are different from local galactic abundances which are thought to be similar to photospheric abundances.

1. INTRODUCTION. Gamma-ray emission from solar flares consists of lines from nuclear reactions and continuum primarily from relativistic electron bremsstrahlung (1,2). These gamma rays are produced in thick-target (3) interactions of energetic particles with ambient gas, most likely in the chromosphere or the transition region. A particularly good gamma-ray spectrum has been observed (4) by the gamma-ray spectrometer (GRS) on SMM from the April 27, 1981 flare. This spectrum shows several narrow lines: at 6.13, 4.44, 1.78, 1.63, 1.37 and 0.85 MeV from deexcitations of ^{16}O, ^{12}C, ^{28}Si, ^{20}Ne, ^{24}Mg and ^{56}Fe, respectively, at 2.22 MeV from neutron capture, at 0.51 MeV from positron annihilation and at ~0.45 MeV from α-α fusion. While earlier work (5,6) predicted that these should be the strongest lines, the observed line ratios are inconsistent (4) with our calculations which assume local galactic (7) abundances for the ambient gas (see Table 1). These local galactic abundances are believed (7) to be similar to photospheric abundances.

2. ANALYSIS. We have calculated deexcitation spectra resulting from thick-target nuclear reactions. These spectra, binned into photon energy channels j defined in ref.(6), can be expressed as $\sum_\ell n(\ell)A(j,\ell)$, where $n(\ell)$ is the abundance of element ℓ (with ℓ defined in Table 1) and $n(\ell)A(j,\ell)$ is the contribution of interactions of all the energetic particles with this element. To these spectra we add bremsstrahlung, the neutron capture line and positron annihilation radiation. For the bremsstrahlung we assume a power law with adjustable index, for the neutron capture we take an infinitely-narrow line at 2.223 MeV and for the

annihilation radiation we assume an infinitely-narrow line at 0.511 MeV along with the orthopositronium continuum corresponding to 67% of the positrons annihilating via positronium. We transform the photon spectra into pulse-height spectra using a numerical model of the detector response which will be presented elsewhere. The total pulse-height spectrum can then be written as $\rho(i) = \sum_\ell n(\ell)\bar{A}(i,\ell) + \bar{A}b(i) + \bar{A}n(i) + \bar{A}p(i)$, where i denotes pulse-height channel number, $\bar{A}(i,\ell)$ is the partial pulse-height spectrum of element ℓ, and $\bar{A}b(i)$, $\bar{A}n(i)$ and $\bar{A}p(i)$ are the bremsstrahlung, neutron capture and positron annihilation pulse-height spectra. We derive the abundances by comparing $\rho(i)$ to the observed pulse-height spectrum and varying the $n(\ell)$'s and $\bar{A}b$, $\bar{A}n$ and $\bar{A}p$ until a best fit is obtained. We only consider one isotope for each element except for C, Ne and Mg, for which we include the contributions of ^{13}C, ^{22}Ne and ^{26}Mg but with fixed isotopic ratios (8).

The partial spectra $\bar{A}(i,\ell)$ depend on the energetic-particle composition, spectrum and angular distribution. The particle composition that we use is given in Table 1. Because in the solar atmosphere interactions amongst nuclei heavier than He are expected to be negligible and because no gamma-ray lines are produced in p-p or p-α interactions, the $\bar{A}(i,\ell)$'s for $\ell>2$ depend only on the energetic protons and α-particles and consist mostly of narrow lines. For the same reason, $\bar{A}(i,1)$ depends only on the energetic C and heavier nuclei and consists mostly of broad lines. $\bar{A}(i,2)$ depends on the energetic α-particles and heavier nuclei and consists of the narrow feature at ~0.45 MeV in addition to broad lines. The dominant contribution to the total pulse-height spectrum is from the $\bar{A}$'s with $\ell>2$. The contributions of $\bar{A}$ with $\ell=1$ and 2 are relatively small, since in a thick target the interactions of the heavier nuclei are supressed by the Z^2/A dependence of the Coulomb energy loss. In addition, a good fit of the calculated pulse-height spectrum to the observed spectrum can only be achieved if the observed narrow lines are adequately accounted for. As just mentioned, the narrow lines are produced mostly by the energetic protons and α-particles. Thus, uncertainties in the abundances of the energetic heavy nuclei relative to each other and relative to the protons do not significantly affect the determination of ambient C and heavier element abundances. The ambient H abundance, however, does depend on the ratio of energetic heavy nuclei to protons and therefore cannot be determined reliably. Information on the ambient He abundance is obtained primarily by fitting the ~0.45 MeV feature and therefore depends on the α/p ratio which is also very uncertain. This uncertainty, however, does not significantly affect the heavy element abundance determinations as long as the α/p ratio is not much larger than ~0.1.

For the energy spectrum of the April 27, 1981 flare we use a Bessel function with $\alpha T = 0.02$, a value close to the average αT determined (3) for several flares using the 2.22 to 4-7 MeV fluence ratio or the high-energy neutron arrival-time profile. We cannot use either method for this flare because the 2.22 MeV line was strongly attenuated owing to the location of the flare on the solar limb and no neutrons were observed. Our calculations, however, indicate that variations in the spectrum do not affect the abundance determinations significantly. The angular distribution of the energetic particles affects the shapes and central energies of the lines, but since the Doppler shifts of the

narrow lines are not expected to exceed the energy resolution of the SMM/GRS detector, we assume that the energetic particles are isotropic.

3. RESULTS. The abundances deduced by optimizing the fit of the calculated spectrum to the data are given in Table 1. This optimization method is discussed in the accompanying paper. Here we derive values of reduced χ^2, χ^2_ν, from the comparison of the gamma-ray abundances shown in Table 1 with both the local galactic and coronal abundances. We have renormalized the gamma-ray abundances using multiplicative factors determined by minimizing χ^2_ν. For the local galactic case, this factor is 1.4, leading to $\chi^2_\nu = 3.6$ ($\nu = 11$). This implies that the gamma-ray abundances are different from the local galactic abundances. For the coronal case, the factor is 1.1 and $\chi^2_\nu = 1.1$ implying that the gamma-ray and coronal abundances are consistent within the errors. The closed circles in Figures 1 and 2 show the ratios of the renormalized gamma-ray abundances to the mean local galactic and coronal abundances. The error bars reflect the 1-σ errors of the gamma-ray abundances. The open boxes represent the errors in the local galactic and coronal abundances.

With the renormalization that we have adopted, the principal difference between the gamma-ray and the local galactic abundances is the underabundance of C and O in the gamma-ray sample. The Fe, Si, Mg and Ne abundances in the two samples are in good agreement, but the statistical errors for Ca, S, Al and N and the systematic error for He (due to the uncertain α/p ratio) are too large to permit a quantitative conclusion. As discussed above, the gamma-ray determination of the H abundance is also subject to a large systematic error. A similar supression of C and O has been found (7) in the coronal abundances relative to the local galactic abundances (which are thought to be similar to photospheric abundances). It has been pointed out that this supression may be caused by charge-dependent mass transport from the photosphere to the corona. Since the photosphere is collisionally ionized at a relatively low temperature, the transport could depend on the first ionization potentials of the elements. While the gamma-ray sample probably pertains to the chromosphere or transition region, similar fractionation effects could be influencing these sites as well. However, if the Ne abundance in the photosphere (where it cannot be measured) is the same as in the local galactic sample, then the difference between the gamma-ray and photospheric abundances must be due to additional processes, because correlation with first ionization potential alone would predict a lower Ne abundance than that derived here.

4. REFERENCES

1. Ramaty, R. et al., 1983, Solar Physics, 86, 395.
2. Chupp, E. L., 1984, Ann. Rev. Astron. Astrophys., 22, 359.
3. Murphy, R. J. and Ramaty, R., 1985, Adv. in Space Res., 4, 127.
4. Forrest, D.J.,1983, in Posi.-Elec. Pairs in Astrop., AIP, NY, p.3.
5. Lingenfelter, R. E. and Ramaty, R., 1967, in High-Energy Nuclear Reactions in Astrophysics, Benjamin, NY, p.99.
6. Ramaty, R., et al., 1979, Ap. J. (Supp), 40, 487.
7. Meyer, J. P., 1985, Ap. J. (Supp), 57, 173.
8. Cameron, A. G. W., 1982, in Essays in Nuc. Astrop., Cambridge, p.23.

5. ACKNOWLEDGEMENTS. We would like to acknowledge discussions with E. L. Chupp and the rest of the GRS team, as well as with R. E. Lingenfelter. The work of DJF was supported by NASA, contract NAS 5-28609.

TABLE 1

Elemental Abundances

ℓ	Element	Local Galactic	Corona	Energetic Particles	Abundances from Gamma Rays
1	H	2.71×10^6 (1.1)	2.55×10^6 (1.4)	8.66×10^5	$(5.61\pm3.49)\times10^5$
2	He	2.60×10^5 (1.25)	2.50×10^5 (3.0)	5.86×10^4	$(1.92\pm0.25)\times10^5$
3	C	1260(1.26)	600(3.0)	270	288± 50
4	N	225(1.41)	100(1.7)	75	117± 91
5	O	2250(1.25)	630(1.6)	600	422± 62
6	Ne	325(1.50)	90(1.6)	85	199± 27
7	Mg	105(1.03)	95(1.3)	144	68± 25
8	Al	8.4(1.05)	7(1.7)	8	-15± 52
9	Si	100(1.03)	100(1.3)	100	100± 28
10	S	43(1.35)	22(1.7)	19	48± 83
11	Ca	6.2(1.14)	7.5(1.5)	7	17± 15
12	Fe	88(1.07)	100(1.5)	99	76± 18

Local galactic and coronal abundances from ref.(7). The quantities in parantheses are multiplicative errors, f. We take m(f-1) as an estimate for a 1-σ error about the mean value m. For the energetic particles, p/α and p/O are the same as those of ref.(8) and C through Fe relative to O or Si are similar to the mass-unbiased solar energetic particle abundances of ref.(7). The gamma-ray abundance errors are 1 σ.

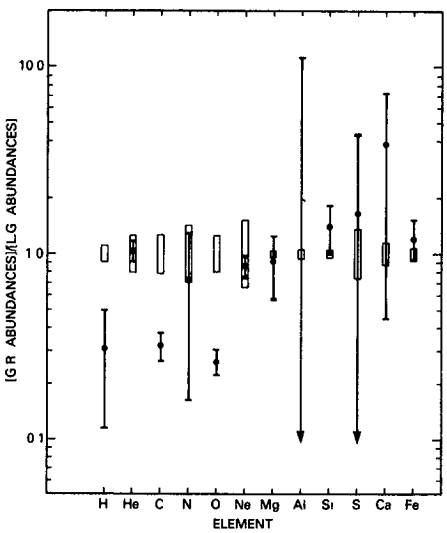

Figure 1. Ratios of renormalized gamma-ray abundances to local galactic abundances (closed circles).

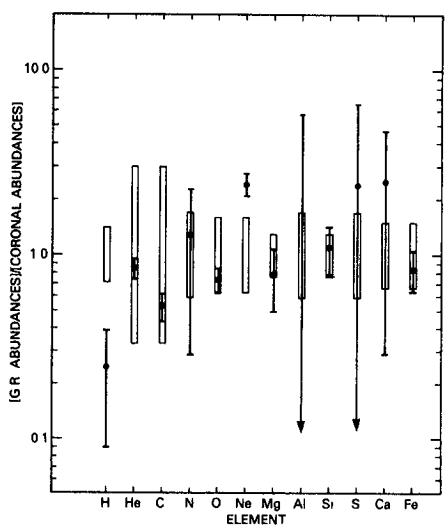

Figure 2. Ratios of renormalized gamma-ray abundances to coronal abundances (closed circles).